Medical Science

25(118), December, 2021

Flow cytometric assessment of nivolumab and/or epigallocatechin-3-gallate on cancer stem cells of DMBA induced hamster buccal pouch carcinoma

To Cite:
Al-Dosoki MA, Abd-Alhafez AAA, Omar AMZ, Zouair MGA. Flow cytometric assessment of nivolumab and/or epigallocatechin-3-gallate on cancer stem cells of DMBA induced hamster buccal pouch carcinoma. Medical Science, 2021, 25(118), 3206-3221

Author Affiliation:
[1]Assistant Lecturer, Oral and Dental Pathology Department, Faculty of Dental Medicine (Boys- Cairo), Al-Azhar University, Egypt
[2]Lecturer, Oral and Dental Pathology Department, Faculty of Dental Medicine (Boys- Cairo), Al-Azhar University, Egypt
[3]Assistant Professor, Department of Clinical Pathology, South Egypt Cancer Institute, Assiut University, Egypt
[4]Professor, Oral and Dental Pathology Department, Faculty of Dental Medicine (Boys-Cairo), Al-Azhar University, Egypt

✉**Corresponding author**
Assistant Lecturer, Oral and Dental Pathology Department, Faculty of Dental Medicine (Boys- Cairo),
Al-Azhar University, Egypt
Email: dentistelagouz@gmail.com, mohamedalaa.9@azhar.edu.eg

Peer-Review History
Received: 06 October 2021
Reviewed & Revised: 08/October/2021 to 26/November/2021
Accepted: 28 November 2021
Published: December 2021

Peer-review Method
External peer-review was done through double-blind method.

Mohamed Alaa Al-Dosoki[1]✉, **Ahmed Abd-Alshakor Abd-Alhafez**[2], **Asmaa Mohamed Zahran Omar**[3], **Mohamed Gomaa Attia Zouair**[4]

ABSTRACT

The aim of the present study was to investigate the effect of nivolumab and/or epigallocatechin-3-gallate (EGCG) on cancer stem cell(s) ($CSC_{(s)}$) of DMBA induced hamster buccal pouch squamous cell carcinoma (HBPSCC). *Material and methods*: fifty Syrian male hamsters were divided into five group(s) ($G_{(s)}$), 10 each. GI: negative control, left untreated. The right pouches of those in GII, GIII, GIV and GV were painted with DMBA (3times /a week/ 14 weeks). GII: positive control, not received other treatment. GIII was injected with intraperitoneally (IP) with nivolumab only, while GIV with IP with EGCG only, whereas GV with IP (combination of nivolumab and EGCG). After termination of the experiment, gross observation was recorded, the animals were euthanized, and all pouches were surgically excised and bisected. The first piece was prepared for H & E stain and immunohistochemical (IHC) staining utilizing CD68 and CD3. The other piece was used for flow cytometric (FCM) assessment for identification and sorting of CSCs using CD44 & CD24 antibodies. Then, apoptosis assay of the sorted CSCs was employed. *Results:* gross observations, H & E stain, IHC and FCM results revealed some variability throughout the treated Gs (GIII-GV) compared to those observed in GII. CSCs sorting, CD44+, CD24-& CD44+, CD24+ revealed high significant difference between GII and Gs: GIII- GV (p value < 0.001). The sorted CSCs apoptosis recorded highly significant difference between GII and other Gs {(GIII- GV) (p value < 0.001)}. *Conclusion:* combination of EGCG-nivolumab significantly inhibits tumor progression and induces apoptosis in CSCs of HBPSCC.

Keywords: HBP carcinoma, EGCG, nivolumab, CSC.

1. INTRODUCTION

Oralcancer is a multifactorial illness that arises because of the interplay of lifestyle, environmental, genetic and epigenetic factors (Mello et al., 2019). It has been found that, oral carcinogenesis induced by 7,12- dimethylbenz(a) anthracene (DMBA) in golden Syrian hamsters is an accepted and well recognized experimental model for studying biochemical, histopathological, immunohistochemical (IHC) and molecular alteration (Manoharan et al., 2010). Unfortunately, oral squamous cell carcinoma (OSCC)is associated with high morbidity and mortality, although great progress has been made in diagnosis and treatment strategies, the 5-year survival rate of OSCC sufferers remains disappointingly low, which may be due to poor drug effectiveness, metastatic development and resistance (Ghantous et al., 2018; Yanamoto et al., 2018).

It has been found that,cancer stem cell(s) (CSC(s)) held the key to unlocking effective strategies to curb initiation and growth of several malignant neoplasms (de Moraes et al., 2017). CSCs are defined as ''cancer root cells'' and have the ability to self-renew and proliferate into heterogeneous malignant stem cells and tumor cells that form the mass of the tumor (Ingangi et al., 2019). The frequency of CSC varies broadly among various tumor types (<0.1% - 43%) (Kloskowski et al., 2020; Zahran et al., 2020; Zahran et al., 2019; Gunduz et al,. 2020). It is believed that, difference in the percentage of CSCs inside a tumor could be related to change in methodology, such as different cell surface markers used to isolate CSCs (Rich et al., 2016). CSCs also display a high drug efflux property, resulting in resistance to anticancer drugs. Furthermore, a favorable microenvironment for CSCs usually includes hypoxia and acidic conditions (pH 6.8 : 7) (Ingangi et al., 2019; Prager et al,. 2019), which can induce altered gene expression and lead to increase in angiogenesis, stemness, and drug efflux transporters. CSCs are plastic and express cellular-specific markers [CD44, CD133, transforming growth factor-beta (TGF-b), etc.] (Lytle et al., 2018; Gordeeva et al., 2019; Steinbichler et al., 2020). Therefore, targeted therapies and diagnostics involving CSCs are considered a unique and promising choice for effective cancer treatment through the targeting of tumor specific features (Han et al., 2020).

It has been found that, targeted therapy and immune checkpoint inhibition were evolved and stay carried out inOSCC patients (Ferris et al., 2016). Several immunotherapeutic modalities have been approved for treatment of OSCC, including immune checkpoint blockade (Moy et al., 2017). Programmed death-1 (PD-1) is a checkpoint molecule expressed on T cells, B cells and monocytes. The ligands for PD-1 include PD-L1 and PD-L2. Both ligands are expressed on endothelial and antigen-presenting cells (APC) and activated lymphocytes (de Vicente et al., 2019). It has been found that, OSCC tissues produce PD-L1 through an abnormal PD-1 signaling pathway, which leads to tumor immunosuppression (Zandberg & Strome, 2014). Immune checkpoint inhibitors targeting the PD-1/PD-L1 axis have been approved for treatment of different cancer types, including non-small-cell lung cancer (NSCLC), renal and hepatocellular carcinomas (Balar & Weber, 2017). Among the drugs that target PD-1, nivolumab (Opdivo) and pembrolizumab (Keytruda), that have been officially agreed by FDA for OSCC patients with recurrence or metastasis who are cisplatin-resistant (Polverini et al., 2018).

It has been found that, natural products could bring a new hope for chemoprevention and treatment of cancer due to less harmful effect on normal cells. This other modality has been used to treat different types of cancers (Yallapu et al., 2013). EGCG which is a natural product, was found to be the most abundant catechin in green tea (Koch et al., 2018). EGCG attracted significant research interest due to its beneficial health effects including anti-oxidation (Cavet et al., 2011) and anti-tumorigenesis activity (Xiang et al., 2016). EGCG inhibit CSCs of NSCLC, prostate and hepatocellular carcinomas, CSCs are targets of EGCG for cancer prevention and therapy (Fujiki et al., 2017). Nevertheless, it has been appreciated that EGCG displays an intriguing effect in adjuvant therapy and prevention of recurrence. As reported, EGCG reduced the recurrence by 51.6% in patients with colorectal adenoma after polypectomy (Fujiki et al., 2015). EGCG together with cisplatin or oxaliplatin increased the therapeutic efficacy in colorectal cancer (Hu et al., 2015).

Hence, the main target of the present study was to assess the effects of nivolumab and/or EGCG on CSCs of DMBA induced hamster buccal pouch (HBP) carcinoma. The assessment was based on the animal's general health examinations, HBP gross observations, histological tumor tissue changes, IHC examinations and flow cytometric studies.

2. MATERIAL AND METHODS

This study was carried out in the Animal Research Unit of the Faculty of Pharmacy, Cairo, Boys, Al-Azhar University. The study is part of a research work started on October 2019 and ended in January 2021.

Chemicals

DMBA (0.5%) was obtained from Sigma-Aldrich Company, dissolved in paraffin oil. Nivolumab (BMS-936558, ONO-4538, or MDX1106, trade name Opdivo; Bristol-Myers Squibb, Princeton, NJ, USA); Nivolumab was prepared by dissolving in 0.9% sodium

chloride (10 mg/ml). EGCG (E4268) was purchased from Sigma Aldrich (St. Louis, MO, USA). EGCG was prepared by direct dissolving the crystalline compound in 0.9% sodium chloride injection (10 mg/ml).

Animals

Fifty Syrian male hamsters five weeks old, weighing 80-120g was obtained from the animal house, Cairo University, Cairo, Egypt. The experimental hamsters were placed in standard boxes with sawdust bedding under controlled environmental conditions of humidity (30-40%), temperature (20 ± 2°C), and light (12-h light/12-h dark). All experimental animals were supplied with standard diet and water ad libitum. A healthy hamster had normal, smooth gait, bright, clear eyes, healthy skin and soft, shiny coat that's free of dry patches, parasites, cuts and swellings. Their mouths not have any cuts, or scrabs.

Sample size

Based on Duzgun et al., (2017) research, a sample size of 10 in each group, in the current study, will have an 80% power to detect a difference between means of 0.53 with a significance level (alpha) of 0.05 (two-tailed) at 95% confidence intervals. In 80% (the power) of those experiments, the p value will be less than 0.05 (two-tailed) so the consequences can bedeemed "statistically significant". In the ultimate 20% of the experiments, the distinction between means will be deemed "not statistically significant". Report created by GraphPad StatMate 2.00.

Experimental design

After a week of adaptation, the animals weresplitrandomly into five group(s) (G(s)), 10 each. While the animals in GI (negative control) were, left untreated, the right pouches of those in GII, GIII, GIV and GV were painted with the 0.5% DMBA in liquid paraffin using a number 4 camel's hair brush, 3times a week for 14 weeks (Vinoth & Kowsalya, 2018). After that, the animalsin GII (positive control) not received other treatment while those in GIII (nivolumab) were injected intraperitoneally (IP) by insulin syringe with nivolumab (200 μL on days 7, 10, and 13) (Selby et al., 2016), on day 22, the animals were euthanized (Sanmamed et al., 2015). The animals in GIV (EGCG) were injected IP with EGCG (10mg/kg / twice a week/ 4 weeks), while those in GV (EGCG - nivolumab) were injected IP with nivolumab and EGCG with doses and administration method similar to those introduced in single treatments.

General health examinations

During the experiment, the changes in the animal's general health were recorded. Hamsters with illness or disease exhibitedany of these signs if they were coping: anorexia, quietness, crowded in a corner, sneezing, diarrhea, discharge from the nose or eyes, wetness around the tail, wheezing and hair loss.

After termination of the experiment, gross observations were recorded (mucosal thickness, exudation, ulcers, and tumors.), the animals were euthanized, the right cheek pouch excised and bisected with one piece of the fresh tissue in saline in order to be examined by fluorescence-activated cell sorting (FACS) and the other piece of the fresh tissue, fixed in 10% neutral buffered formalin, routinely processed and embedded in paraffin blocks in order to be examined histologically and immunohistochemically. The firstpiece of the fresh tissue was mechanically digested, suspended and conjugated with fluorophore-antibodies (CD44 & CD24) of CSCs surface marker to be sorted using FACS.

Histopathological examinations

Tissue sections of 4μm thickness were cut from paraffin blocks using rotary microtome, mounted on glass slides, processed, and stained with hematoxylin and eosin (H&E) for light microscopic examination.

Measurement of the Depth of Invasion (DOI)

DOI was measured for all surgical specimens based on the H & E slide. DOI was measured from the basal layer of the surface epithelium to the deepest point of tumor invasion. It has further been classified as less invasive ≤5 mm, moderate invasive 6–10 mm, and deeply invasive ≥10 mm, according to American joint committee on cancer (AJCC) (Faisal et al., 2018) (Fig.1). DOI was measured using Leica QWIN V3 image analyzer computer system (Switzerland), controlled by Leica QWIN V3 software. This was done in Oral and Dental Pathology Department, Faculty of Dental Medicine (Boys-Cairo), Al-Azhar University, Egypt.

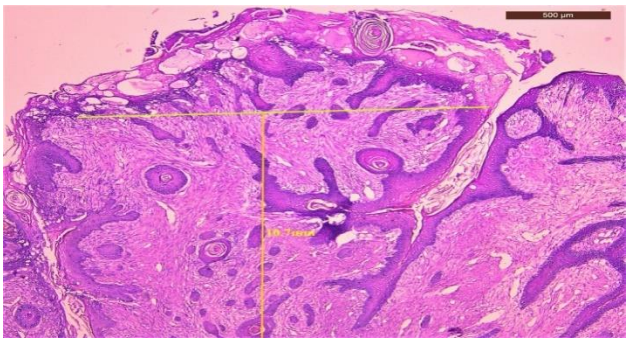

Figure 1 Photograph of measuringthe depth of invasion, the greatest invasion was measured by dropping a "plumb line" from the horizon to the deepest invasive nest.

Immunohistochemical examination

Other tissue sections were cut at 4μm and puton positive charged slides for the application of standard labeled streptavidin- biotin method to demonstrate the expression of CD68 & CD3 antibodies. The sections were deparaffinized in xylene and rehydrated through graded ethanol (100%, 95 % and 70 %) each run for 5 minutes. Slides were washed in distilled water then in phosphate buffered saline (PBS), each for 5 minutes. Endogenous peroxidase activity was blocked using 3% solution of hydrogen peroxide (H_2O_2) in methanol for 30 minutes at room temperature. Slides were then washed in PBS. Slides were then immersed in plastic jars containing 200 ml of citrate buffer (pH 6). The jars were put in microwave at maximum power at 100°C for 3 intervals, each one 5 minutes. Slides were left atroom temperature to coal gradually. Slides were then washed in distilled water followed by PBS for 5 minutes.

Tissue sections were received one or two drops of the primary antibodies (CD68 or CD3) in adilution of 1:100 and incubated in a humid chamber at room temperature overnight. Slides were then washed in distilled water, followed by PBS for 5 minutes. Biotinylated secondary antibody was added and incubated at room temperature for 30 minutes. Tissue sections were then washed in PBS for5 minutes. One or two drops of peroxidase-labeled streptavidin were applied for 30 minutes at room temperature then washed in PBS. The tissue sections were received DAB for 2-4 minutes to develop color, followed by putting in distilled water. Tissue sections were counter stained using Mayer's hematoxylin for sixty seconds, after that, slides washed in tap water. The slides were placed in two changes of 95% alcohol followed by two changes of absolute alcohol, each for 3 minutes then mounted with DPX and covered with plastic covers in order to be examined. Negative controls were prepared by omitting the primary antibody. Human tonsillar tissues were used as positive controls for CD3 (Fig.2A), while spleen tissues were used as positive controls for CD68 (Fig.2B).

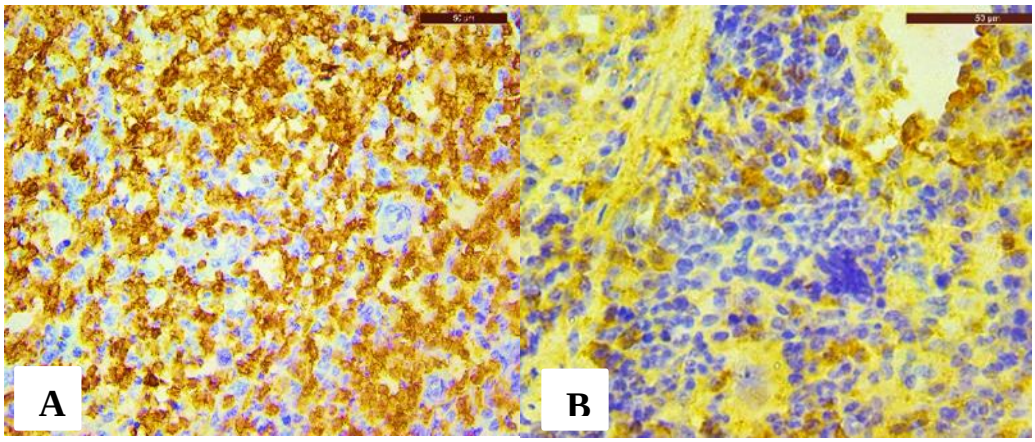

Figure 2A Photomicrograph of tonsillar tissue (positive control) showing CD3+ve lymphocyte (stained brown); (Streptavidin biotin peroxidase X 400). (Fig. 2B): Photomicrograph of spleen tissue (positive control) showing CD68+ve cells in the lymph nodule (stained brown) (Streptavidin biotin peroxidase X 400).

The immunostained slides were analyzed using light microscope to evaluate the frequency of positive cases and the localization of immunostaining inside the tissues. In addition, image analysis computer system was used to assess area percentage of CD3 positive cells of the immunostaining. Assessment of the macrophage number was conducted by the positive staining CD68 cell

count under a light microscope. At first, 3 regions with densest macrophage in the cancer, i.e., the hot spot region, were selected under a low power lens (10×10), then counting was conducted under a high-power lens (10 ×40), and a mean value was chosen for statistical analysis (Weber et al., 2017). This was done in Oral and Dental Pathology Department, Faculty of Dental Medicine (Boys-Cairo), Al-Azhar University, Egypt.

Flow cytometric detection and isolation of CSCs

Isolation and characterization of CSCs

Mechanical dissociation of OSCC

The tumor mass was placed into a 35 mm petri dish with 3 mL of PBS. Tumor specimen was extensively washed (2 to 3 times) in PBS to remove blood and debris.The specimen was held steady with tissue forceps, and with the back of a no. 22 scalpel blade, the specimen was scraped descending, and away, such that cells are go through the tumor mass into the dish. As cells were broken from the tumor mass, threads of connective tissue (CT) were isolated, and were removed from the collection. The scrapping was continued until the tumor massis too small to catch to have a large population in the dish. The tumor solution became pipetted up and down 3 to 5 min with a 5-ml disposable pipet. Then, the solution was placed into a 15-ml conical tube. The remaining sample was centrifuged at 2500 rpm for 2 minutes at 4°C. The media was aspirated off and the cellular pellet was resuspended in PBS in an appropriate volume needed for FACS analysis (Dobbin & Landen, 2013).

Apoptosis assay of all specimen cells

Annexin V-Fluorescein isothiocyanate (FITC)/Propidium iodide (PI) Apoptosis Detection Kit (Catalog No: E-CK-A211, Elabscience Biotechnology, Texas, USA) was used. The cells were washed and placed in 100 μL of the Annexin V-conjugate binding buffer to which 10 μL of FITC-conjugated Annexin and 10 μl of PI were added. After incubation for 15 min, 400 μL of the binding buffer was added. Cells were analyzed by the usage of a flow cytometer (BD FACSC alibur, San Jose, CA, USA) with BD FACSDiva 7.0 software. This was done in the FCM Unit, Clinical Pathology Department, South Egypt Cancer Institute, Assiut University, Egypt. The profile graph, presented the Annexin V FITC parameter along the X-axis and the PI parameter along the Y-axis. Four different populations of cells were distinguished, in a clockwise direction starting from the upper left quadrant: cells that were stained with PI (necrotic), those that have both bound to annexin-V FITC and been labeled with PI (late apoptotic), and those that have bound to annexin-V FITC only (early apoptotic), those that have been unlabeled (viable cells). Of these four kinds of cell modes, early and late apoptosis were calculated among the cell population.

Identification and sorting of CSCs

The cellular pellet was suspended in PBS in an appropriate volume. 10 μL of Phycoerythrin-labeled anti-mouse CD24(PE-CD24) monoclonal antibody (clone M1/69; Elabscience Biotechnology, Texas, USA) and 10 μL of Allophycocyanin -labeled anti-mouse CD44 (APC-CD44) monoclonal antibody (clone G44–26; BD Biosciences, CA, USA) was added to the sample, concentration 1: 100.The samples were incubated with the antibodies for 30 minutes at 4°C, protected from light. The cells were resuspended in PBS and the expressions of CD24 and CD44 was quantitatively measured by FACSCalibur flow cytometer (BD Biosciences) with BD FACSDiva 7.0 software. Cell populations were sorted using FACSCalibur flow cytometer. Firstly,Cells were gated based on light scatters,then by positive gating of CD44+ CD24- and CD44+ CD24+ cells (Han et al., 2014).

Apoptosis assay of the sorted CSCs

Apoptosis was detected in the sorted CSCs

Statistical analysis

The results were recorded as the mean standard ± standard deviation (SD) and statistically analyzed. A one-way analysis of variance (ANOVA) was performed using SPSS version 17.0 for windows. The differentiation between more than two different groups with quantitative data and parametric distribution was done by using ANOVA then, post hoc analysis using LSD test. The p value was considered significant as the following: $p > 0.05$: non-significant, $p < 0.05$: significant and $p < 0.001$: highly significant.

3. RESULTS

Gross observations

GI showed no gross changes, no hair loss, no skin ulcerations, normal pale pink colorof the HBP with neither pathological nor inflammatory changes. Their buccal pouch lengths were about 5 cm for all hamsters (Fig.3A). GII showed marked hair loss, pouch depth decrease, skin ulcers and marked debilitation of all animals. Animal's pouches showed large exophytic growths with pronounced vascularity and the pouch length ranged from 1.5-2cm with distal necrotic end (Fig.3B). GIII and GIV showed slight improvement in the general health (table 1). The length of the pouches was about 2.5cm with reduction of distal necrosis. Slight decrease in size of the papillomatous lesions was observed (Fig.3C & D). GV showed marked improvement in general health of animals. There was a considerable increase of the pouch's length to about 3.5cm with no distal necrosis. There was marked decrease in the size of exophytic masses in this groups when compared to animals treated with nivolumab or EGCG only (Fig.3E).

Table 1 Common clinical findings observed in the studied groups

features	Groups				
	GI	GII	GIII	GIV	GV
anorexia	-	+++	++	++	+
quietness	-	+++	++	++	+
corner crowding	-	+++	++	++	+
sneezing, wheezing, and/or discharge from the nose or eyes,	-	+++	++	++	+
wetness around the tail, diarrhea	-	+++	++	++	+
hair loss	-	+++	++	++	+
Gross observations					
Papillomatous lesion	-	+++	++	++	+
Pouch length	5 cm	1.5-2cm	2.5cm	2.5cm	3.5cm
Ulcers	-	+++	++	++	+
Exudation	-	+++	++	++	+
Tumors	-	100 %	50 %	50 %	30%

– = no change; + = mild; ++ = moderate; +++ = severe

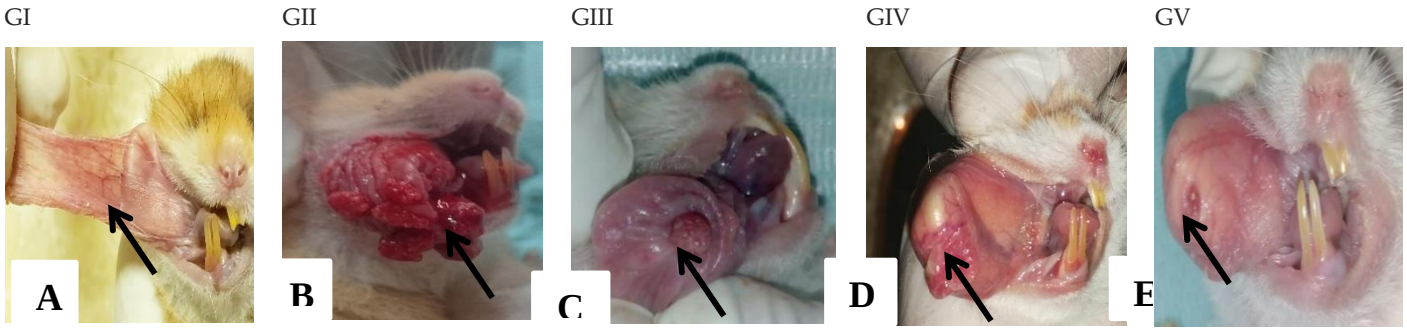

Figure 3 A: HBP of GI showing normal buccal pouch mucosa which appeared pink in color with smooth surface (arrow). (Fig.3B): HBP of GII showing multiple exophytic papillary tumor masses surrounded with bleeding areas (arrow). (Fig.3C): HBP of GIII showing small tiny elevation with absence of ulceration and bleeding (arrow). (Fig.3D): HBP of GIV showing small size nodule with absence of ulceration and bleeding (arrow). (Fig.3E): HBP of GV showing marked decrease in the size of tumor masses with absence of ulceration and bleeding (arrow).

Histological findings

GI revealed normal thin stratified squamous epithelium, consists of two to three layers of squamous cells exhibiting slight keratinization (i.e.; one row of basal cells and one, two or three rows of spinous with thin keratinization cells and absence of rete ridges. Sub-epithelial CT and muscular layer were seen (Fig.4A). GII revealed well to moderate differentiated SCC in the form of large papillomatous lesions with invading islands of epithelium into underlying C.T (DOI=10.7mm) with marked chronic inflammatory cells and necrotic mass at the distal end of pouch. The invading malignant cells showed basilar hyperplasia, loss of polarity, hyperchromatism, prominent nucleoli, altered N\C ratio and cellular & nuclear pleomorphism (Fig.4B). GIII and GIV

revealed moderate to severe epithelial dysplasia with areas of topto bottom changes or carcinoma in situ (CIS) were seen in five hamsters while the other five hamsters showed superficial invasion of malignant cells in the form of well differentiated SCC which was limited to the nodules only, not extended to deeper areas (DOI=1.7-1.8mm). There was reduction of the distal necrosis, inflammatory infiltration and increase amount of collagen fibers (Fig.4C & D). GV revealed moderate to severe epithelial dysplasia were seen inseven hamsters (epithelium had focal areas of dysplasia represented as hyperchromatism, altered N/C ratio; cellular & nuclear pleomorphism, prominent nucleoli, as well as multiple group cell keratinization's while three hamsters showed well differentiated SCC which was juxta-epithelial and not extended to the deeper C.T (DOI=0.8mm) with increased amount of keratin formation (table 2). The C.T showed marked decrease of distal necrosis, inflammatory infiltration and increase thickness of striated muscle layer and the tumor masses were mostly replaced by proliferated fibrous tissue with more collagen deposition (Fig.4E).

Table 2 Histopathologicalchanges in HBP of controls and treated groups

Features	Groups				
	GI	GII	GIII	GIV	GV
Irregular epithelial stratification	-	+++	++	++	+
Basilar hyperplasia	-	+++	++	++	+
loss of polarity	-	+++	++	++	+
Individual cell keratinization	-	+++	++	++	+
keratin pearls	-	+++	++	++	+
Nuclear pleomorphism	-	+++	++	++	+
Cellular pleomorphism	-	+++	++	++	+
Abnormal mitotic figures	-	+++	++	++	+
Hyperchromatism	-	+++	++	++	+
Abnormal N/C ratio	-	+++	++	++	+
Inflammatory infiltration	-	+++	++	+	+
Increase amount of collagen fibers	-	-	++	++	+++
DOI	-	10.7mm	1.8mm	1.7mm	0.8mm
Epithelial histological changes					
Milddysplasia	-	+++	+++	+++	10%
Moderatedysplasia	-	+++	10%	10%	30%
Severe dysplasia	-	+++	20%	20%	20%
CIS	-	+++	20%	20%	10%
SCC	-	Well (50 %) Moderate (50 %)	Well (50 %)	Well (50 %)	Well (30 %)

– = no change; + = mild; ++ = moderate; +++ = severe.

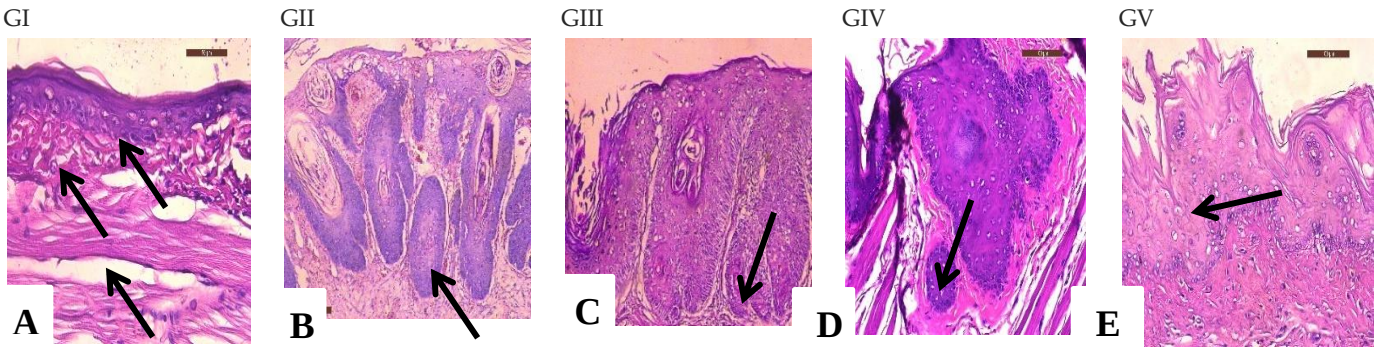

Figure 4 A: H&E stain of GI showing: epithelium consists of two tofour layers, superficial squamous cells exhibiting keratinization, flattened rete ridges, C.T layer, muscular layer and deep layer of loose areolar connective tissue (arrow). (X200) (Fig.4B): H&E stain of GII showing well differentiated SCC with deep invasion of multiple tumor islands into the underlying connective tissue and sub-epithelial inflammatory infiltrates (arrow). (X100). (Fig.4C): H&E stain of GIII showing well differentiated SCC (superficial invasion) (arrow). (X200). (Fig.4D): H&E stain of GIV showing well differentiatedSCC (superficial invasion) (arrow). (X200). (Fig.5E): H&E stain of GV showing severe dysplasia with hyperkeratosis (arrow) (X200).

Immunohistochemical findings

CD68

Numerous CD68-positive cells were observed in all studied cases. A cytoplasmatic expression pattern was found. Macrophage infiltration was rarely found in GI; in other groups, CD68+ cells distributed mostly in the stroma, in or around the neoplastic cell nests. Representative images of CD68+ cells are shown in (Fig.5A-C). There was highly significant difference between GI & GII (pvalue < 0.001). There was significant difference between GII & GIII as well as between GII & GIV (pvalue = 0.018, 0.002 respectively). There was highly significant difference between GII & GV (pvalue < 0.001) (Table 3, Fig .6).

CD3

Numerous CD3-positive cells were observed in all studied cases. The immunohistochemical positive reaction was detected as brown deposits at membrane of lymphocytes. CD3-positive cells were rarely identified in GI. In other groups, CD3+ cells were detected in both tumor center and invasive margin. Representative images of CD3+ cells are shown in (Fig.5D-F). There was highly significant difference between GI& GII (pvalue < 0.001). There was significant difference between GII & GIII (pvalue =0.001). There was highly significant difference between GII when compared to either GIV or GV (pvalue < 0.001) (Table 3, Fig .6).

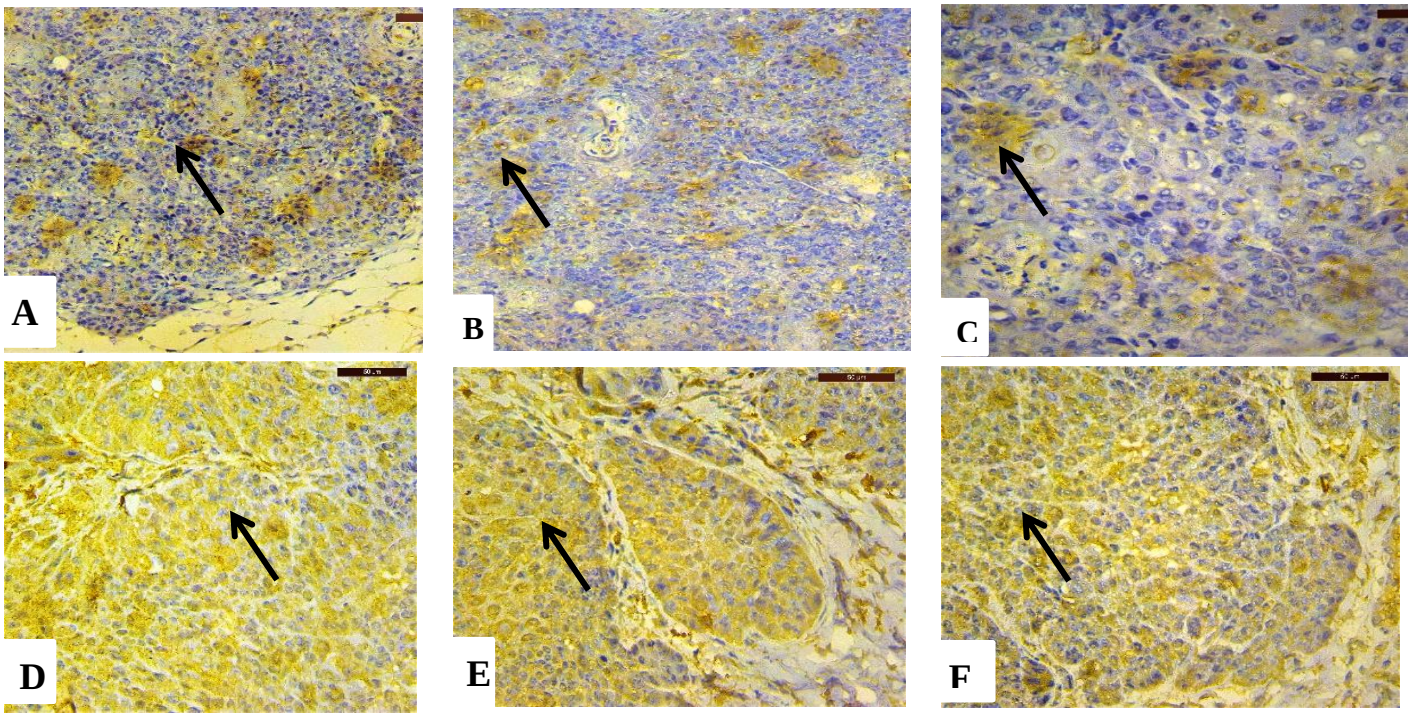

Figure 5 (A-C): IHC expression CD68 in OSCC (representative images) (Streptavidin biotin peroxidase). (Fig.5D-F): IHC expression CD3 in OSCC (representative images) (Streptavidin biotin peroxidase).

Table 3 Comparison between studied group's asregard CD68 and CD3.

		GI (n = 10)	GII (n = 10)	GIII (n = 10)	GIV (n = 10)	GV (n = 10)	F	P-value
CD68	Mean	2.0	40.6	32.2	29.3	26.5	35.7	< 0.001 HS
	±SD	2.8	11.8	7.0	8.1	5.9		
CD3	Mean	3.0	43.6	32.9	31.6	29.7	51.5	< 0.001 HS
	±SD	3.3	9.0	6.2	8.9	3.3		

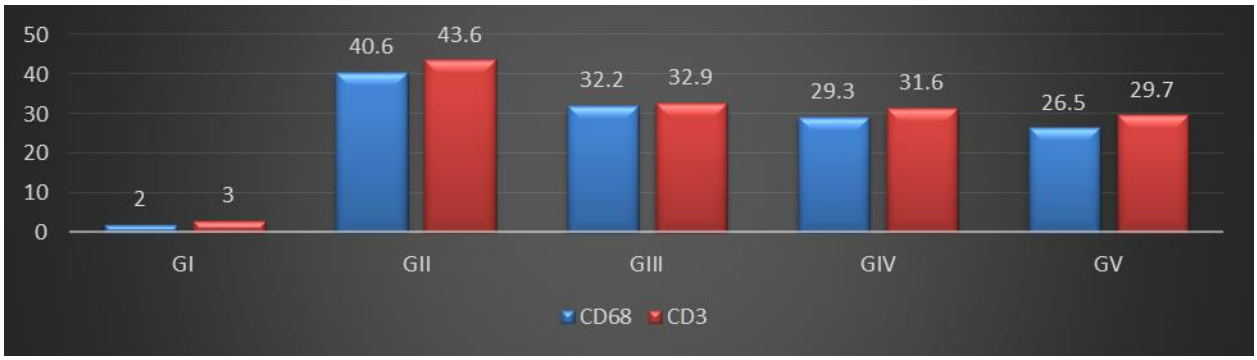

Figure 6 Bar chart representing mean count and area% results of CD68 and CD3 respectivly.

Detection of Apoptosis of all specimen cells by flow cytometry

GI, 1.72% of the cells underwent apoptosis while the cells of GII resulted in 22.8% apoptosis. In the study Gs, GIII resulted in 53.7% apoptosis while GIV resulted in 44.1% apoptosis. GV resulted in 67.7% apoptosis. There was highly significant difference between GII and other treatment Gs (GIII, GIV and GV), (pvalue < 0.001). There was significant difference between GV and GIII (pvalue= 0.001). There was highly significant difference between GV and GIV (pvalue < 0.001) (Table 4, Fig. 7).

Table 4 Comparison between studied groups as regard apoptosis of all specimen cells and apoptosis of CSC

		GII (n = 10)	GIII (n = 10)	GIV (n = 10)	GV (n = 10)	F	P-value
Apoptosis of all specimen cells	Mean	22.8	53.7	44.1	67.7	168.5	< 0.001 HS
	±SD	3.3	7.1	9.8	11.8		
Apoptosis of CSC	Mean	1.3	35.7	21.8	44.6	15.8	< 0.001 HS
	±SD	0.7	14.1	7.3	18.2		

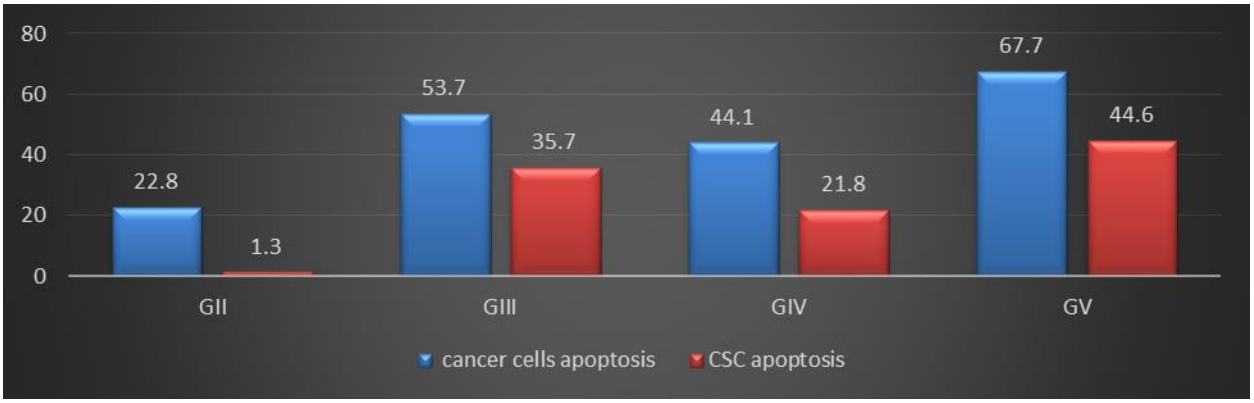

Figure 7 Bar chart representing mean results of apoptosis of cancer cells and CSC.

Isolation and characterization of CSCs

Two phenotypic subpopulations were separated, CD44+/CD24- and CD44+/CD24+. The percentage of CD44+/CD24- cells in GI, GII, GIII, GIV and GV was 0.005%, 1.33%, 0.25%, 0.28% and 0.15%, respectively. While the percentage of CD44+/CD24+ cells in GI, GII, GIII, GIV and GV was 0.001%, 0.11%, 0.05%, 0.04% and 0.02%, respectively. There was highly significant difference between GI & GII (p value < 0.001). There was highly significant difference between GII the treated Gs {(GIII- GV, (p value > 0.05)}. In CD44+ CD24-, There was significant difference between GV when compared to either GIII or GIV, p value= 0.041 and 0.044 respectively. In CD44+ CD24+, There was significant difference between GV when compared to either GIII or GIV, p value= 0.019 and 0.039 respectively (Table 5, Fig. 8).

Table 5 comparisons between studied groups as regard CD44+ CD24- & CD44+CD24+

		GI (n = 10)	GII (n = 10)	GIII (n = 10)	GIV (n = 10)	GV (n = 10)	F	P-value
CD44+ CD24-	Mean	0.005	1.33	0.25	0.28	0.15	159.4	< 0.001 HS
	±SD	0.002	0.21	0.17	0.07	0.08		
CD44+ CD24+	Mean	0.001	0.11	0.05	0.04	0.02	26.2	< 0.001 HS
	±SD	0.002	0.04	0.03	0.01	0.02		

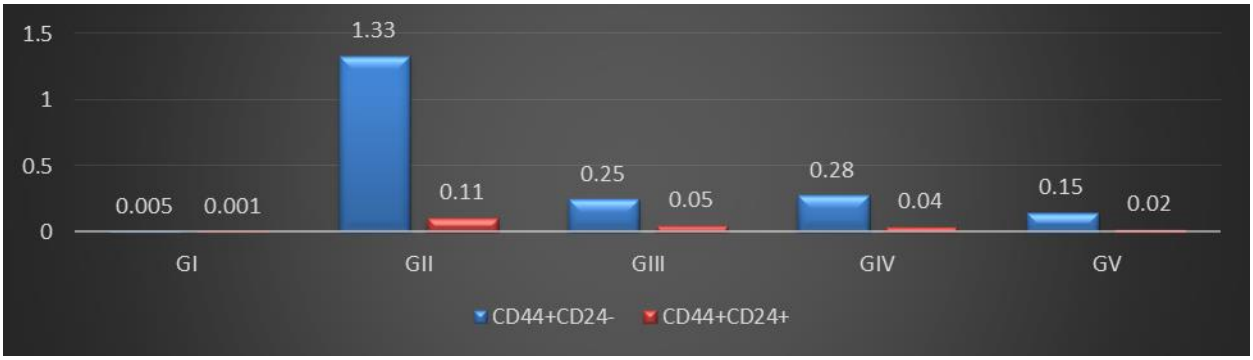

Figure 8 Bar chart representing mean results of CD44+ CD24- and CD44+ CD24+

Apoptosis of CSCs

GI, 26.5% of the cells underwent apoptosis while the cells of GII resulted in 1.3% apoptosis. In the study Gs, GIII resulted in 35.7% apoptosis while GIV resulted in 21.8% apoptosis. GV resulted in 44.6% apoptosis. There was highly significant difference between GII and other treated Gs {(GIII- GV) (pvalue < 0.001)}. There was highly significant difference between GV when compared to either GIII or GIV, pvalue < 0.001 (Table 4, Fig. 7).

4. DISCUSSION

To our knowledge, in the open English literatures, this was the first study to evaluate the effect of nivolumab and/or EGCG on CSCs of DMBA induced HBP carcinoma. The results of animal's general health examinations, HBP gross observations, H&E stain, IHC examinations and FCM assessment, revealed variable observations. In the present study, GI showed no observable abnormalities of the HBP with neither pathological nor inflammatory changes. After animal's euthanization, the buccal pouches length was about 5cm for all hamsters with normal histological structures (Bruna et al., 2017; Casto et al., 2013) reported the same findings.

In the current study, GII showed marked hair absence, pouch depth reduction, skin ulcers and noticeable debilitation of all animals. Animal's pouches showed large exophytic growths with pronounced vascularity and the pouch length (1.5-2cm) which was decreased compared to GI due to necrosis in the distal end of the pouch. These observations are mainly due to the strong toxic DMBA effect (El-Hossary et al., 2018). By using H & E stain, a development of various patterns of invasive SCC 100% (well differentiated and moderately differentiated) were seen which extended to deeper areas of C.T (DOI=10.7mm). This is in consistence with that shown by other researchers (Sophia et al., 2016; Manoharan et al., 2015; Hassan et al., 2020). These findings may be referred to higher level of reactive oxygen species (ROS) inside the cell during DMBA application which may be attributed to repeated exposures to tumor promoters create a chronic inflammatory state with a sustained release of ROS, which results in chronic oxidative stress. Free radicals and non-radical ROS such as H2O2 released by phagocytic cells can result ininjury, such as breaks of DNA strand, mutations, sister chromatid exchanges, protein alterations and lipid peroxidation, to adjacent epithelial cells. In addition, protein alterations induced by free radicals/ROS can have an impact on DNA repair mechanism, transcriptional status, apoptosis and cell signaling (Rundhaug and Fischer, 2010). This is in consistence with that shown by other studies (Manimaran et al., 2017; Selvasundaram et al., 2018). Contrastingly, in the study conducted by Hussein et al., (2018), only 66.67% of the hamsters developed oral tumors, and that could be attributed to the different solvent material.

In the current study, IHC staining of HBP mucosa in GII with CD68 and CD3 antibodies showed highly significant increasing expression compared to GI (p value < 0.001). These results are consistent with the results of Lo Muzio et al., (2010) whom reported that, the most expressed molecule of tumor microenvironment was CD68, followed by CD45, CD20 and CD3. FCM results revealed that, in GII only 22.8% undergo apoptosis of highly proliferative cancer tissue which may be attributed to that, DMBA have a

stimulatory effect on Bcl-2 which makes the removal of genetically modified cells difficult, favoring the accumulation of new mutations, which can result in the appearance of cells with malignant phenotype. These results are in line with Sophia et al., (2018) whom stated that, Bcl-2 has the capacity of interrupting the apoptosis process both in the initial and final phases because this protein stabilizes the potential of the mitochondria membrane when forming heterodimers with Bax.

In the present study, GIII showed slight improvement in the animal's general health. The pouch length (2.5cm) was decreased compared to GII due to decrease of the inflammatory infiltration and distal necrosis. A relatively slight decrease in size of the papillomatous lesions was observed. These findings conflicted on H & E staining in which five hamsters revealed different degrees of epithelial dysplasia {(moderate (10%), severe (20%) or CIS (20%)} while the other five hamsters showed superficial invasion of well differentiated SCC (50 %), not extended to deeper areas (DOI=1.8mm). As shown by IHC staining of HBP mucosa in GIII with CD68 and CD3 antibodies showed significant difference compared to GII (p value = 0.018, 0.001 respectively). FCM results revealed that, OSCC treatment with nivolumab resulted in higher apoptosis (53.7%) than GII with high significance difference between GIII and GII (p value <0.001). These results may be attributed to that; nivolumab is immune check point inhibitor capable of specific inhibition of PD-1 signal that was sufficient to reduce the invasive lesions. This is in line with (Chen et al., 2018; Lee and Sunwoo, 2014; Tada et al., 2020). Lee and Sunwoo, (2014) explained that, blocking the tumor-infiltrating lymphocytes (TILs) with anti-PD-L1 and anti-PD-1 antibodies partially restored interferon (IFN)-g secretion by the TILs incubated with the CD44+ cells, indicating that CD44+ cells have immunosuppressive features which mediated by the PD-L1/PD-1 axis. These results indicated that, PD-L1 expression on CSCs may function as a mechanism by which CSCs evade immunosurveillance and provide a cause for targeting the PD-1 axis.

In the present study, GIV showed almost the same results as GIII. FCM results revealed that OSCC treatment with EGCG displayed higher apoptosis (44.1%) than GII and lower than GIII with high significance difference between GIV and GII (p value <0.001) and significance difference between GIV and GIII (p value = 0.017). These results are in agreement with (Yoshimura et al., 2019; Chen et al., 2011; Hwang et al., 2013) which reported the growth suppressive effects of EGCG on OSCC. Yoshimura et al., (2019) reported that, EGCG diminished tumor growth, induces apoptosis and halt the cell cycle in OSCC cells, resulting in antiproliferative impacts both in vitro and in vivo: in a mouse show, noteworthy development hindrance of the OSCC tumor was watched in EGCG-treated mice. Other mechanism for EGCG inhibitory effect was proposed by Rawangkan et al., (2018) in which EGCG inhibited PD-L1 expression in NSCLC, induced by both IFN-γ and epidermal growth factor (EGF) in addition, EGCG reduced PD-L1 mRNA expression about 30% in melanoma cells. This is in consistence with that shown by Xu et al., (2018) whom reported that, apigenin (flavonoids as EGCG) restricted melanoma growth through suppression of PD-L1 on both neoplastic cells and APCs. In brief, EGCG is an alternative immune checkpoint inhibitor that inhibits PD-L1 expression.

In the current study, IHC staining of HBP mucosa in GIV with CD68 antibody showed significant difference compared to GII (p value = 0.002), while IHC staining of HBP mucosa in GIV with CD3 antibody showed highly significant increasing expression compared to GII (p value < 0.001). These results are in line with Luo et al., (2020) whom found that, EGCG could attenuate CD68 and CD3 expression as the common pharmacological characteristics of EGCG antioxidant and anti-inflammatory effects which modulates the oxidative stress and infiltration of immune cells.

In the present study, GV as a combination group showed marked improvement in animal's general health compared to nivolumab G or EGCG G alone. There was a considerable increase of the pouch's length (3.5cm) due to marked decrease of distal necrosis and inflammatory infiltration. Also, there was marked decrease in the size of exophytic masses in GV when compared to the animals treated with nivolumab or EGCG only. These findings conflicted on H & E staining which revealed different degrees of epithelial dysplasia {mild (10%), moderate (30%), severe (20%) or CIS (10%)} in addition to well differentiated SCC (30%) which was juxta-epithelial and not extended to the deeper C.T (DOI=0.8mm) with increased amount of keratin formation. The C.T showed marked increase thickness of striated muscle layer and the tumor masses were mostly replaced by proliferated fibrous tissue with more collagen deposition. IHC staining of HBP mucosa in GV with CD68 and CD3 antibodies showed highly significant difference compared to GII (p value < 0.001). FCM results revealed that, OSCC treatment with EGCG resulted in higher apoptosis (67.6%) than GII and nivolumab G or EGCG G alone with high significance difference between GV either with GII or GIV (p value < 0.001) and significance difference between GV and GIII (p value < 0.05). These findings reflected the beneficial effect of combining nivolumab with EGCG in order to achieve these positive results. These results may be attributed to the synergetic effect between EGCG and nivolumab as PD-L1/PD-1 immune checkpoint inhibitor as block the interactions of PD-1 molecules on T cells with PD-L1 molecules on tumor cells or APCs. This is in consistence with (Lin et al., 2018; Vento et al., 2019). Targeting the PD-1/PD-L1 axis has become a promising therapeutic strategy in cancer therapy, through preventing the escape of neoplastic cells from the immune surveillance and helping the host's immune system to reattack the neoplastic cells (Yang et al., 2016).

CSCs are considered as the main target in current cancer therapy. CD44 and CD24 have been identified as CSC surface markers in OSCC. The percentage of CD44+/CD24- and CD44+/CD24+ cells in GII were 1.33% and 0.11% respectively, with highly significant difference between GII and GI (p value < 0.001). This is in consistence with (Ghuwalewala et al., 2016; Todoroki et al., 2016; Han et al., 2014). Ghuwalewala et al., (2016) revealed that, CD44+CD24- cells is able to form larger spheres than CD44+CD24+within a few days, indicative of its ability to undergo asymmetric division and self-renewal powers. In vitro, CD44+CD24- cells found to be more migratory and invasive, although these cells did not proliferate faster, but under clonal conditions, could result in holoclone-like colonies, a typical property of CSCs. Conversely, Han et al., (2014) found that, CD24+/CD44+ cells were growing rapidly, more invasive in vitro and more tumorigenic in vivo compared to CD24-/CD44+ cells. In addition, CD24+/CD44+ cells were found to be tougher against chemotherapeutic drugs compared to CD24-/CD44+ cells. These findings indicate that CD24+/CD44+ cells may represent CSCs in OSCC.

By FCM, this study found that, only 1.3% of CSC undergoes apoptosis which may attribute to that CSC increases the level of Bcl-2 relative to Bax (i.e., a lower Bax/Bcl-2 ratio) promotes the mitochondrial retention of cytochrome C and resulted in reduced apoptotic cell death. There was highly significant decreasing expression compared to GI (p value < 0.001). These results are in accordance with Todoroki et al., (2016), Ghuwalewala et al., (2016) and Chen & Wang, (2019). Todoroki et al., (2016) found that, anti-apoptotic genes such as Bcl-2 and CFLAR were more highly expressed in the CD44+/CD24− cells using real-time PCR assays. Wang & Bourguignon, (2006) revealed that, CD44 can interact with hyaluronan to promote phospholipase C-mediated intracellular Ca2+ mobilization in order to prevent apoptotic effects caused by cisplatin.

In the present study, the percentage of CD44+/CD24- and CD44+/CD24+ cells in GIII were 0.25% and 0.05% respectively with highly significant difference between GIII and GII (p value < 0.001). FCM results revealed that, OSCC treatment with nivolumab resulted in higher apoptosis of CSCs (35.7%) than GII with high significance difference between GIII and GII (p value < 0.001). This is in consistence with that shown by Bommireddy et al., (2020) and Tada et al., (2020). Tada et al., (2020) findings suggested that, the induction of an effective antitumor immune response by nivolumab treatment presumably allows the concentration of circulating tumor cells (CTCs) to display the CSCs phenotype due to lysis of non-CSC tumor cells. Although CSCs are competent of self-renewal and differentiation (Nassar & Blanpain, (2016), CSCs can evade immune surveillance by reducing immunogenicity and immune suppressive activity compared with their non-CSC cancer cells (Clara et al., 2020; Servat & Rosell, 2015; Qian et al., 2015; Maccalli et al., 2014). Wang et al., (2017) detected more T cell activation in oral lesions in mice treated with anti-PD-1, resulted in release of granzyme B which may contribute to induce apoptosis.

In the present study, the percentage of CD44+/CD24- and CD44+/CD24+ cells in GIV were 0.28% and 0.04% respectively with highly significant difference between GIV and GII (p value < 0.001). This is in consistence with that shown by Pan et al., (2016) and Kumazoe et al., (2017). Our result verifies that, EGCG can target CSCs which explained by Chen et al., (2012) in their study on human breast CSCs, EGCG inhibit cellular proliferation, suppress CD44+ /CD24- cells and activate AMPK signaling pathway. FCM results revealed that, OSCC treatment with EGCG resulted in higher apoptosis of CSCs (21.8%) than GII and lower than GIII with significance difference between GIV either with GII or GIII (p value =0.002, 0.032 respectively). This is in consistence with that shown by Lee et al., (2013) and Kang et al., (2013). EGCG are thought to function as powerful radical scavengers, in particular, under increased oxidative stress conditions. Moreover, EGCG can induce apoptosis in different ways, such as affecting the apoptotic proteins (Bax, Bcl-2, Bcl-XL) and regulator proteins of cell cycle (cyclins, CDKs) (Negri et al., 2018).

In the present study, the percentage of CD44+/CD24- and CD44+/CD24+ cells in GV were 0.15% and 0.02% respectively with highly significant difference between GV and GII (p value < 0.001). In CD44+ CD24-, there was significant difference between GV when compared to either GIII or GIV (p value= 0.041 and 0.044 respectively). In CD44+ CD24+, there was significant difference between GV when compared to either GIII or GIV (p value= 0.019 and 0.039 respectively). These findings showed the synergetic effect between EGCG and nivolumab as PD-L1/PD-1 immune checkpoint inhibitor. This is in line with that shown by Lee et al., (2016) whom concluded that, because CD44+ cells have the capacity for long-term self-renewal and tumor initiation, the immunosuppression conferred by PD-L1 expression may augment the resilience of these cells and allow them to selectively suppress and evade immune responses. Their findings provide an explanation for the better responses observed with PD-1/ PD-L1 blockade and provide a reason for the use of PD-1/ PD-L1 blockade as adjuvant therapy after surgical removal of OSCC tumors with high-risk for relapse.

By FCM, the present study revealed that, OSCC treatment with combination of EGCG-nivolumab resulted in higher apoptosis of CSCs (44.6%) than GII and nivolumab G or EGCG G alone with high significance difference between GV and GII (p value < 0.001). There was highly significant difference between GV when compared to either GIII or GIV (p value < 0.001). This is in line with that shown by Lee et al., (2013) whom found that, EGCG not only kill differentiated cancer cells but could also kill CSCs. EGCG attenuates OSCC CSC via down-regulation the Notch signaling pathway. EGCG and cisplatin together reduced OSCC CSC viability

and suppressed ABCC2 & ABCG2 expression, which have been involved in the treatment of CSC resistance. Interestingly, EGCG administered concomitantly with cisplatin significantly inhibited tumor development and initiated apoptosisin a xenograft model.

5. CONCLUSION

In conclusion; the present research revealed that, the combination of EGCG-nivolumab could inhibit tumor progression and induces apoptosis not only in non-CSC OSCC but also in CSC OSCC. This combination significantly improves the therapeutic efficacy. On the other hand, CSCs can enhance tumor progression either by CSCs immunoediting that can survive in an immunocompetent host or by posting conditions that facilitate neoplastic growth within the tumor microenvironment. Therefore, specific targeting of CSCs by immunotherapeutic modalities may lead to more functional and better helpful comes about within the future. Regarding CD44 CD24, further studies are necessary to provide a specific phenotype in OSCC, like those of other organs. Finally, EGCG and nivolumab as an anticancer is a promising novel targeted therapy for treating OSCC.

Ethical Approval

Ethical approval cleared by ethical committee of Faculty of Dental Medicine (Boys- Cairo), Al-Azhar University, Egypt (Ethical Code No. 35/38-11-10-21).

Funding

This study has not received any external funding.

Conflict of Interest

The authors declare that there are no conflicts of interests.

Data and materials availability

All data associated with this study are presented in the paper.

REFERENCES AND NOTES

1. Balar A, Weber J. PD-1 and PD-L1 antibodies in cancer: current status and future directions. Cancer Immunol Immunother 2017; 66(5):551-64.
2. Bommireddy R, Munoz L, Kumari A, Huang L, Fan Y, Monterroza L,Pack C, Ramachandiran S, Reddy S, Kim J, Chen Z, Saba N, Shin D, Selvaraj P. Tumor membrane vesicle vaccine augments the efficacy of anti-PD1 antibody in immune checkpoint inhibitor-resistant squamous cell carcinoma models of head and neck cancer. Vaccines 2020; 8(2):182.
3. Bruna F, Rodríguez M, Plaza A, Espinoza I, Conget P. The administration of multipotent stromal cells at precancerous stage precludes tumor growth and epithelial dedifferentiation of oral squamous cell carcinoma. Stem Cell Res 2017; 18:5-13.
4. Casto B, Knobloch T, Galioto R, Yu Z, Accurso B, Warner B. Chemoprevention of oral cancer by lyophilized strawberries. Anticancer Res 2013; 33(11):4757-66.
5. Cavet M, Harrington K, Vollmer T, Ward K, Zhang J. Anti-inflammatory and anti-oxidative effects of the green tea polyphenol epigallocatechin gallate in human corneal epithelial cells. Mol Vis 2011; 17:533-42.
6. Chen D, Pamu S, Cui Q, Chan T, Dou Q. Novel epigallocatechin gallate (EGCG) analogs activate AMP-activated protein kinase pathway and target cancer stem cells. Bioorg Med Chem 2012; 20(9):3031-37.
7. Chen D, Wang C. Targeting cancer stem cells in squamous cell carcinoma. Precis Clin Med 2019; 2(3):152-65.
8. Chen N, Chu C, Kuo H, Chou Y, Lin K, Hsieh S. Epigallocatechin-3 gallate inhibits invasion, epithelial–mesenchymal transition, and tumor growth in oral cancer cells. J agric food chem 2011; 59(8):3836-44.
9. Chen Y, Li Q, Li X, Ma D, Fang J, Luo L, Liu X, Wang X, Lui V, Xia J, Cheng B, Wang Z. Blockade of PD-1 effectively inhibits in vivo malignant transformation of oral mucosa. Oncoimmunology 2018; 7(2):e1388484.
10. Clara J, Monge C, Yang Y, Takebe N. Targeting signalling pathways and the immune microenvironment of cancer stem cells—A clinical update. Nat Rev Clin Oncol 2020; 17(4):204-32.
11. de Moraes F, Lourenço S, Ianez R, de Sousa E, Silva M, Damascena A, Kowalski L, Soares F, Camillo C. Expression of stem cell markers in oral cavity and oropharynx squamous cell carcinoma. Oral Surg Oral Med Oral Pathol Oral Radiol 2017; 123(1):113-22.
12. de Vicente J, Rodríguez T, Rodrigo J, Blanco V, Allonca E, García J. PD-L1 expression in tumor cells is an independent unfavorable prognostic factor in oral squamous cell

carcinoma. Cancer Epidemiol Biomarkers Prev 2019; 28(3):546-54.
13. Dobbin Z, Landen C. Isolation and characterization of potential cancer stem cells from solid human tumors—potential applications. Curr Protoc Pharmacol 2013; 63(1):14.28.
14. Duzgun O, Sarici I, Gokcay S, Ates K, Yılmaz M. Effects of nivolumab in peritoneal carcinamatosis of malign melanoma in mouse model. Acta Cir Bras 2017; 32(12):1006-12.
15. El-Hossary W, Hegazy E, El-Mansy M. Topical chemopreventive effect of thymoquinone versus thymoquinone loaded on gold nanoparticles on dmba-induced hamster buccal pouch carcinogenesis (immunohistochemical study). Egypt Dent J 2018; 64(4):3523-33.
16. Faisal M, Abu Bakar M, Sarwar A, Adeel M, Batool F, Malik K, Jamshed A,Hussain R. Depth of invasion (DOI) as a predictor of cervical nodal metastasis and local recurrence in early stage squamous cell carcinoma of oral tongue (ESSCOT). PloS one 2018; 13(8):e0202632.
17. Ferris R, Blumenschein G, Fayette J, Guigay J, Colevas A, Licitra L, Harrington K, Kasper S, Vokes E, Even C, Worden F, Saba N, Docampo L, Haddad R, Rordorf T, Kiyota N, Tahara M, Monga M, Lynch M, Geese W, Kopit J, Shaw J, Gillison M. Nivolumab for recurrent squamous-cell carcinoma of the head and neck. N Engl J Med 2016; 375(19):1856-67.
18. Fujiki H, Sueoka E, Rawangkan A, Suganuma M. Human cancer stem cells are a target for cancer prevention using (−)-epigallocatechin gallate. J Cancer Res Clin Oncol 2017; 143(12):2401-12.
19. Fujiki H, Sueoka E, Watanabe T, Suganuma M. Synergistic enhancement of anticancer effects on numerous human cancer cell lines treated with the combination of EGCG, other green tea catechins, and anticancer compounds. J Cancer Res Clin Oncol 2015; 141(9):1511-22.
20. Ghantous Y, Bahouth Z, El-Naaj I. Clinical and genetic signatures of local recurrence in oral squamous cell carcinoma. Arch Oral Biol 2018; 95:141-48.
21. Ghuwalewala S, Ghatak D, Das P, Dey S, Sarkar S, Alam N, Panda C, Roychoudhury S. CD44highCD24low molecular signature determines the cancer stem cell and EMT phenotype in oral squamous cell carcinoma. Stem Cell Res 2016; 16(2):405-17.
22. Gordeeva O. TGFβ family signaling pathways in pluripotent and teratocarcinoma stem cells' fate decisions: balancing between self-renewal, differentiation, and cancer. Cells 2019; 8(12):1500.
23. Gunduz M, Gunduz E, Tamagawa S, Enomoto K, Hotomi M. Identification and chemoresistance of cancer stem cells in HPV-negative oropharyngeal cancer. Oncol lett 2020; 19(1):965-71.
24. Han J, Fujisawa T, Husain S, Puri R. Identification and characterization of cancer stem cells in human head and neck squamous cell carcinoma. BMC cancer 2014; 14(1):173.
25. Han J, Won M, Kim J, Jung E, Min K, Jangili P, Kim J. Cancer stem cell-targeted bio-imaging and chemotherapeutic perspective. Chem Soc Rev 2020; 49(22):7856-78.
26. Hassan M, El-Hossary W, Hanafi R. Anti-inflammatory Thymoquinone and Muscle Regeneration in the Hamster Buccal Pouch-Induced Dysplasia. J Oral Health Dent Sci 2020; 4:302.
27. Hu F, Wei F, Wang Y, Wu B, Fang Y, Xiong B. EGCG synergizes the therapeutic effect of cisplatin and oxaliplatin through autophagic pathway in human colorectal cancer cells. J Pharmacol Sci 2015; 128(1):27-34.
28. Hussein A, El-Sheikh S, Darwish Z, Hussein K, Gaafar A. Effect of genistein and oxaliplatin on cancer stem cells in oral squamous cell carcinoma: an experimental study. Alex Dent J 2018; 43(1):117-23.
29. Hwang Y, Park K, Chung Y. Epigallocatechin-3 gallate inhibits cancer invasion by repressing functional invadopodia formation in oral squamous cell carcinoma. Eur J Pharmacol 2013; 715(1-3):286-95.
30. Ingangi V, Minopoli M, Ragone C, Motti M, Carriero M. Role of microenvironment on the fate of disseminating cancer stem cells. Front Oncol 2019; 9:82.
31. Kang S, Lee B, Lee S, Baek S, Shin Y, Kim C. Expression of NSAID-activated gene-1 by EGCG in head and neck cancer: involvement of ATM-dependent p53 expression. J Nutr Biochem 2013; 24(6):986-99.
32. Kloskowski T, Jarząbkowska J, Jundziłł A, Balcerczyk D, Buhl M, Szeliski K, Bodnar M, Marszałek A, Drewa G, Drewa T, Pokrywczyńska M. CD133 Antigen as a Potential Marker of Melanoma Stem Cells: In Vitro and In Vivo Studies. Stem Cells Int 2020; 2020:8810476.
33. Koch W, Kukula-Koch W, Komsta Ł, Marzec Z, Szwerc W, Głowniak K. Green tea quality evaluation based on its catechins and metals composition in combination with chemometric analysis. Molecules 2018; 23(7):1689.
34. Kumazoe M, Takai M, Hiroi S, Takeuchi C, Yamanouchi M, Nojiri T, Onda H, Bae J, Huang Y, Takamatsu K, Yamashita S, Yamada S, Kangawa K, Takahashi T, Tanaka H, Tachibana H. PDE3 inhibitor and EGCG combination treatment suppress cancer stem cell properties in pancreatic ductal adenocarcinoma. Sci rep 2017; 7(1):1917.
35. Lee S, Nam H, Kang H, Kwon H, Lim Y. Epigallocatechin-3-gallate attenuates head and neck cancer stem cell traits through suppression of Notch pathway. Eur J Cancer 2013; 49(15): 3210-18.

36. Lee Y, Shin J, Longmire M, Wang H, Kohrt H, Chang H, Sunwoo J. CD44+ cells in head and neck squamous cell carcinoma suppress t-cell–mediated immunity by selective constitutive and inducible expression of PD-L1. Clin Cancer Res 2016; 22(14):3571-81.
37. Lee Y, Sunwoo J. PD-L1 is preferentially expressed on CD44+ tumor-initiating cells in head and neck squamous cell carcinoma. J Immuno Ther Cancer 2014; 2(S3):P270.
38. Lin S, Huang G, Cheng L, Li Z, Xiao Y, Deng Q, Jiang Y, Li B, Lin S, Wang S, Wu Q, Yao H, Cao S, Li Y, Liu P, Wei W, Pei D, Yao Y, Wen Z, Zhang X, Wu Y, Zhang Z, Cui S, Sun X, Qian X, Li P. Establishment of peripheral blood mononuclear cell-derived humanized lung cancer mouse models for studying efficacy of PD-L1/PD-1 targeted immunotherapy. MAbs; 2018 ;10(8):1301-11.
39. Lo Muzio L, Santoro A, Pieramici T, Bufo P, Di Alberti L, Mazzotta P, Mazzotta A, Carinci F, Rubini C, Lo Russo L. Immunohistochemical expression of CD3, CD20, CD45, CD68 and bcl-2 in oral squamous cell carcinoma. Anal Quant Cytol Histol 2010; 32(2):70-77.
40. Luo D, Xu J, Chen X, Zhu X, Liu S, Li J, Xu X, Ma X, Zhao J, Ji X. Author Correction:(−)-Epigallocatechin-3-gallate (EGCG) attenuates salt-induced hypertension and renal injury in Dahl salt-sensitive rats. Sci Rep 2020; 10(1):10586.
41. Lytle N, Barber A, Reya T. Stem cell fate in cancer growth, progression and therapy resistance. Nat Rev Cancer 2018; 18(11):669-80.
42. M Yallapu M, Jaggi M, C Chauhan S. Curcumin nanomedicine: a road to cancer therapeutics. Curr Pharm Des 2013; 19(11):1994-2010.
43. Maccalli C, Volontè A, Cimminiello C, Parmiani G. Immunology of cancer stem cells in solid tumours. A review. Eur J Cancer 2014; 50(3):649-55.
44. Manimaran A, Buddhan R, Manoharan S. Emodin downregulates cell proliferation markers during DMBA induced oral carcinogenesis in Golden Syrian Hamsters. Afr J Tradit Complement Altern Med 2017; 14(2):83-91.
45. Manoharan S, Rajasekaran D, Prabhakar M, Karthikeyan S, Manimaran A. Modulating effect of Enicostemma littorale on the expression pattern of apoptotic, cell proliferative, inflammatory and angiogenic markers during 7, 12-dimethylbenz (a) anthracene induced hamster buccal pouch carcinogenesis. Toxicol Int 2015; 22(1):130-40.
46. Manoharan S, VasanthaSelvan M, Silvan S, Baskaran N, Singh A, Kumar V. Carnosic acid: a potent chemopreventive agent against oral carcinogenesis. Chem biol interact 2010; 188(3):616-22.
47. Mello F, Melo G, Pasetto J, Silva C, Warnakulasuriya S, Rivero E. The synergistic effect of tobacco and alcohol consumption on oral squamous cell carcinoma: a systematic review and meta-analysis. Clin Oral Investig 2019; 23(7):2849-59.
48. Moy J, Moskovitz J, Ferris L. Biological mechanisms of immune escape and implications for immunotherapy in head and neck squamous cell carcinoma. Eur J Cancer 2017; 76:152-66.
49. Nassar D, Blanpain C. Cancer stem cells: basic concepts and therapeutic implications. Annu Rev Pathol 2016; 11:47-76.
50. Negri A, Naponelli V, Rizzi F, Bettuzzi S. Molecular targets of epigallocatechin—Gallate (EGCG): A special focus on signal transduction and cancer. Nutrients 2018; 10(12):1936.
51. Pan X, Zhao B, Song Z, Han S, Wang M. Estrogen receptor-α36 is involved in epigallocatechin-3-gallate induced growth inhibition of ER-negative breast cancer stem/progenitor cells. J pharmacol Sci 2016; 130(2):85-93.
52. Polverini P, D'Silva N, Lei Y. Precision therapy of head and neck squamous cell carcinoma. J Dent Res 2018; 97(6):614-21.
53. Prager B, Xie Q, Bao S, Rich J. Cancer stem cells: the architects of the tumor ecosystem. Cell Stem Cell 2019; 24(1):41-53.
54. Qian X, Ma C, Nie X, Lu J, Lenarz M, Kaufmann A, Albers A. Biology and immunology of cancer stem (-like) cells in head and neck cancer. Crit Rev Oncol Hematol 2015; 95(3):337-45.
55. Rawangkan A, Wongsirisin P, Namiki K, Iida K, Kobayashi Y, Shimizu Y, Fujiki H, Suganuma M. Green tea catechin is an alternative immune checkpoint inhibitor that inhibits PD-L1 expression and lung tumor growth. Molecules 2018; 23(8):2071.
56. Rich J. Cancer stem cells: understanding tumor hierarchy and heterogeneity. Medicine 2016; 95(1 Suppl 1):S2-S7.
57. Rundhaug J, Fischer S. Molecular mechanisms of mouse skin tumor promotion. Cancers 2010; 2(2):436-82.
58. Sanmamed M, Schalper K, Onate C, Azpilikueta A, Rodriguez M, Kastresana A, Rodriguez I,Labiano S, Gracia J, Algarra S, Alfaro C, Mazzolini G, Sarno F, Hidalgo M, Korman A, Kunkel M, Melero I. Nivolumab and urelumab enhance antitumor activity of human T lymphocytes engrafted in Rag2−/− IL2Rγnull immunodeficient mice. Cancer Res 2015; 75(17):3466-78.
59. Selby M, Engelhardt J, Johnston R, Lu L, Han M, Thudium K, Yao D, Quigley M, Valle J, Wang C, Chen B, Cardarelli P, Blanset D, Korman A. Preclinical development of ipilimumab and nivolumab combination immunotherapy: mouse tumor models, in vitro functional studies, and cynomolgus macaque toxicology. PLoS One 2016; 11(9):e0161779.
60. Selvasundaram R, Manoharan S, Buddhan R, Neelakandan M, Naidu R. Chemopreventive potential of esculetin in 7, 12-dimethylbenz (a) anthracene-induced hamster buccal

pouch carcinogenesis. Mol Cell Biochem 2018; 448(1-2):145-53.
61. Servat J, Rosell R. Cancer stem cells and immunoresistance: clinical implications and solutions. Transl Lung Cancer Res 2015 ;4(6):689-703.
62. Sophia J, Kowshik J, Dwivedi A, Bhutia S, Manavathi B, Mishra R, Nagini S. Nimbolide, a neem limonoid inhibits cytoprotective autophagy to activate apoptosis via modulation of the PI3K/Akt/GSK-3β signalling pathway in oral cancer. Cell Death Dis 2018; 9(11):1087.
63. Sophia J, Kowshik J, Mishra R, Nagini S. Nimbolide, a neem limonoid inhibits phosphatidyl inositol-3 kinase to activate glycogen synthase kinase-3β in a hamster model of oral oncogenesis. Sci Rep 2016; 6:22192.
64. Steinbichler T, Savic D, Dudás J, Kvitsaridze I, Skvortsov S, Riechelmann H, Skvortsova I. Cancer stem cells and their unique role in metastatic spread. Semin Cancer Biol 2020; 60:148-56.
65. Tada H, Takahashi H, Iwakawa R, Nagata Y, Uchida M, Shino M, Ida S, Mito I, Matsuyama T, Chikamatsu K. Molecular phenotypes of circulating tumor cells and efficacy of nivolumab treatment in patients with head and neck squamous cell carcinoma. Sci Rep 2020; 10(1):21573.
66. Todoroki K, Ogasawara S, Akiba J, Nakayama M, Naito Y, Seki N, Kusukawa J, Yano H. CD44v3+/CD24-cells possess cancer stem cell-like properties in human oral squamous cell carcinoma. Int J Oncol 2016; 48(1):99-109.
67. Vento J, Mulgaonkar A, Woolford L, Nham K, Christie A, Bagrodia A, de Leon A, Hannan R, Bowman I, McKay R, Kapur P, Hao G, Sun X, Brugarolas J. PD-L1 detection using 89 Zr-atezolizumab immuno-PET in renal cell carcinoma tumorgrafts from a patient with favorable nivolumab response. J Immunother Cancer 2019; 7(1):144.
68. Vinoth A, Kowsalya R. Chemopreventive potential of vanillic acid against 7,12-dimethylbenz(a)anthracene-induced hamster buccal pouch carcinogenesis. J Cancer Res Ther 2018; 14(6):1285-90.
69. Wang J, Xie T, Wang B, William W, Heymach J, El-Naggar A, Myers J, Caulin C. PD-1 blockade prevents the development and progression of carcinogen-induced oral premalignant lesions. Cancer Prev Res 2017; 10(12):684-93.
70. Wang S, Bourguignon L. Hyaluronan and the interaction between CD44 and epidermal growth factor receptor in oncogenic signaling and chemotherapy resistance in head and neck cancer. Arch Otolaryngol Head Neck Surg 2006; 132(7):771-78.
71. Weber M, Herold M, Distel L, Ries J, Moebius P, Preidl R, Geppert C, Neukam F, Wehrhan F. Galectin 3 expression in primary oral squamous cell carcinomas. BMC cancer 2017; 17(1):906.
72. Xiang L, Wang A, Ye J, Zheng X, Polito C, Lu J, Li Q, Liang Y. Suppressive effects of tea catechins on breast cancer. Nutrients 2016; 8(8):458.
73. Xu L, Zhang Y, Tian K, Chen X, Zhang R, Mu X, Wu Y, Wang D, Wang S, Liu F, Wang T, Zhang J, Liu S, Zhang Y, Tu C, Liu H. Apigenin suppresses PD-L1 expression in melanoma and host dendritic cells to elicit synergistic therapeutic effects. J Exp Clin Cancer Res 2018; 37(1): 261.
74. Yanamoto S, Umeda M, Kioi M, Kirita T, Yamashita T, Hiratsuka H, Yokoo S, Tanzawa H, Uzawa N, Shibahara T, Ota Y, Kurita H, Okura M, Hamakawa H, Kusukawa J, Tohnai I. Multicenter retrospective study of cetuximab plus platinum-based chemotherapy for recurrent or metastatic oral squamous cell carcinoma. Cancer Chemother Pharmacol 2018; 81(3):549-54.
75. Yang J, Chen J, Wei J, Liu X, Cho W. Immune checkpoint blockade as a potential therapeutic target in non-small cell lung cancer. Expert Opin Biol Ther 2016; 16(10):1209-23.
76. Yoshimura H, Yoshida H, Matsuda S, Ryoke T, Ohta K, Ohmori M, Yamamoto S, Kiyoshima T, Kobayashi M, Sano K. The therapeutic potential of epigallocatechin-3-gallate against human oral squamous cell carcinoma through inhibition of cell proliferation and induction of apoptosis: In vitro and in vivo murine xenograft study. Mol Med Rep 2019; 20(2):1139-48.
77. Zahran A, Abdel-Rahim M, Refaat A, Sayed M, Othman M, Khalak L, Hetta H. Circulating hematopoietic stem cells, endothelial progenitor cells and cancer stem cells in hepatocellular carcinoma patients: Contribution to diagnosis and prognosis. Acta Oncol 2020; 59(1):33-39.
78. Zahran A, Rayan A, Fakhry H, Attia A, Ashmawy A, Soliman A, Elkady A, Hetta H. Pretreatment detection of circulating and tissue CD133+ CD44+ cancer stem cells as a prognostic factor affecting the outcomes in Egyptian patients with colorectal cancer. Cancer Manag Res 2019; 11:1237-48.
79. Zandberg D, Strome S. The role of the PD-L1: PD-1 pathway in squamous cell carcinoma of the head and neck. Oral Oncol 2014; 50(7):627-32.